



Plant egg cell fate determination depends on its exact position in female gametophyte

Yang Sun^a, Xiu Wang^a, Lin Pan^a, Fei Xie^a, Bo Dai^a, Mengxiang Sun^a, and Xiongbo Peng^{a,1}

^aState Key Laboratory of Hybrid Rice, College of Life Sciences, Wuhan University, 430072 Wuhan, China

Edited by Robert L. Fischer, University of California, Berkeley, CA, and approved January 21, 2021 (received for review August 18, 2020)

Plant fertilization involves both an egg cell, which fuses with a sperm cell, and synergid cells, which guide pollen tubes for sperm cell delivery. Therefore, egg and synergid cell functional specifications are prerequisites for successful fertilization. However, how the egg and synergid cells, referred to as the “egg apparatus,” derived from one mother cell develop into distinct cell types remains an unanswered question. In this report, we show that the final position of the nuclei in female gametophyte determines the cell fate of the egg apparatus. We established a live imaging system to visualize the dynamics of nuclear positioning and cell identity establishment in the female gametophyte. We observed that free nuclei should migrate to a specific position before egg apparatus specialization. Artificial changing in the nuclear position on disturbance of the actin cytoskeleton, either in vitro or in vivo, could reset the cell fate of the egg apparatus. We also found that nuclei of the same origin moved to different positions and then showed different cell identities, whereas nuclei of different origins moved to the same position showed the same cell identity, indicating that the final positions of the nuclei, rather than specific nucleus lineage, play critical roles in the egg apparatus specification. Furthermore, the active auxin level was higher in the egg cell than in synergid cells. Auxin transport inhibitor could decrease the auxin level in egg cells and impair egg cell identity, suggesting that directional and accurate auxin distribution likely acts as a positional cue for egg apparatus specialization.

egg cell | synergid cell | cell fate | nuclear position | auxin

Land plants exhibit a complex life cycle that alternates between a diploid sporophytic generation and a reduced, haploid gametophytic generation. In most angiosperms with polygonum-type female gametophytes (FGs), also referred to as embryo sacs, megaspore mother cells undergo meiosis to produce four megaspores. Three of the four megaspores are located at the micropylar end of the sac and degenerate, and only one megaspore, called the functional megaspore, located at the chalazal end, gives rise to an FG. The development process of FGs can be divided into stages FG1 to FG7 (1). Functional megaspores undertake three successive rounds of mitosis to produce eight nuclei. During cellularization, the eight nuclei form seven cells with four cell fates: a female gamete egg cell and two synergid cells in the micropylar end, a large diploid central cell in the central area, and three antipodal cells at the chalazal end (2).

The egg cell and two synergid cells, collectively termed the egg apparatus, are sister cells but with distinct cell fate and function (3, 4). Cell type-specific microarray or transcriptome studies have revealed that egg and synergid cells have distinct gene expression profiles in plants (5–8). The synergid cells have important roles in pollen tube guidance (6, 9, 10) and pollen tube bursting (11–13). The egg cell, as a female gamete, fuses with one sperm cell to give rise to the embryo. In addition, egg cells can activate sperm cells for fertilization (14).

How the egg apparatus differentiates is a critical issue and is a prerequisite for successful fertilization. However, how the egg cell fate is determined and how it becomes distinguishable from its sister, synergid cells remains largely unknown. In past years, several genetic studies have shed light on the specification of the egg apparatus. Some mutants have more than one egg cell in the

embryo sac, such as *eostre*, *wyrd*, *lachesis* (*lis*), *clotho* (*clo/gfa1*), *atropos* (*ato*), and *amp* mutants (15–20). It seems likely that supernumerary egg cells form at the expense of synergid cells, with two nuclei occupying an egg cell position and only one nucleus occupying a synergid cell position. The abnormal positioning of nuclei observed in these mutants suggests that the cell specification of the egg cell and synergid may relate to their nuclear position. However, these earlier conclusions are generally based on indirect effects of mutations in genes with primary functions that are not involved in nuclear positioning in the gametophyte. In addition, whether their egg cell fates are indeed determined by their specific positions in the embryo sac, and whether nuclear position is a cause or a consequence of the egg apparatus specification, remain unknown (21). A direct demonstration of this hypothesis has been lacking, due to the difficulty of manipulating living FGs.

Recently, Susaki et al. (22) used live imaging to visualize the precise dynamics of FG development in *Torenia fourmieri*. After disrupting an immature egg cell with laser, the nucleus of one of the two synergid cells changed position from the micropylar end to the chalazal end and showed reduced LURE2, a synergid marker of gene expression. However, whether the synergid cell showed abnormal position has egg cell fate is unknown.

Here we provide direct evidence for the nuclear position in the embryo sac determining egg cell specification. We established a live imaging system to visualize the dynamics of nuclear positioning and egg apparatus specification in the embryo sac. We reveal that the accurate position is the premise for egg apparatus specification, and that auxin likely acts as a positional cue for egg cell fate determination.

Significance

In a mature female gametophyte of angiosperm, one egg cell and two synergid cells, referred to as the “egg apparatus,” originate from the same functional megaspore. How the egg cell and synergid cells differentiate into distinct cell types has drawn much attention but remains unclear. In this work, a live imaging system was established to visualize nuclear movement and cell specialization in female gametophytes. The final localization of the nuclei before cellularization was found to be critical for determining the cell fates of the egg apparatus. Artificial changes in the nuclear position could produce two functional egg cells. Furthermore, the plant hormone auxin was suggested as a positional cue for egg apparatus specialization.

Author contributions: M.-X.S. and X.P. designed research; Y.S., X.W., L.P., F.X., B.D., and X.P. performed research; X.P. analyzed data; and Y.S., M.-X.S., and X.P. wrote the paper. The authors declare no competing interest.

This article is a PNAS Direct Submission.

Published under the PNAS license.

¹To whom correspondence may be addressed. Email: bobopx@whu.edu.cn.

This article contains supporting information online at <https://www.pnas.org/lookup/suppl/doi:10.1073/pnas.2017488118/-DCSupplemental>.

Published February 17, 2021.

Results

Nuclei Migrate to Specific Positions before Cell Specialization of the Egg Apparatus. FGR7.0 is a marker line with red fluorescent protein (RFP) in the egg cell nucleus, bright green fluorescent protein (GFP) in synergid cell nuclei, and weak yellow fluorescent protein (YFP) in the central cell (Fig. 1A) (23). In mature FGs, the nuclear positions of three types of cells have specific regions: the synergid cell (SC) zone, egg cell (EC) zone, and central cell (CC) zone (Fig. 1B). To investigate the relationship of nuclear position and cell identity in FGs, we developed a marker line, termed nuclear position and cell identity (NPCI), to show the nuclear position and cell identity by crossing the *proRH29::H2B-GFP* marker line with FGR7.0 (*SI Appendix, Fig. S1*). In a previous study, we showed that the *proRH29::H2B-GFP* marker line could clearly label the nuclei of FGs from stage FG1 to stage FG6 (24).

To understand how the nuclei migrate and to determine their position before cell identity establishment or cell type differentiation, we established an in vitro culture system to ensure that the ovules at the four-nucleate FG stage (stage FG4) could develop normally to the cell identity specification stage (stage FG6) (Fig. 1C and D). Combining the aforementioned culture system with confocal microscopy, we developed a live imaging system to visualize the nuclear movement and cell specification in the FG of the NPCI (Fig. 1E). The whole process can be followed in *Movie S1*. In the early four-nucleate FG stage (time 0, stage FG4-1; Fig. 1E-1 and F-1), two nuclei were located horizontally at the micropylar end, and two nuclei were located vertically at the chalazal end. The two nuclei at the micropylar end then turned to a vertical position (stage FG4-2; Fig. 1E-2). At this time point, we named these nuclei A, B, C, and D along the

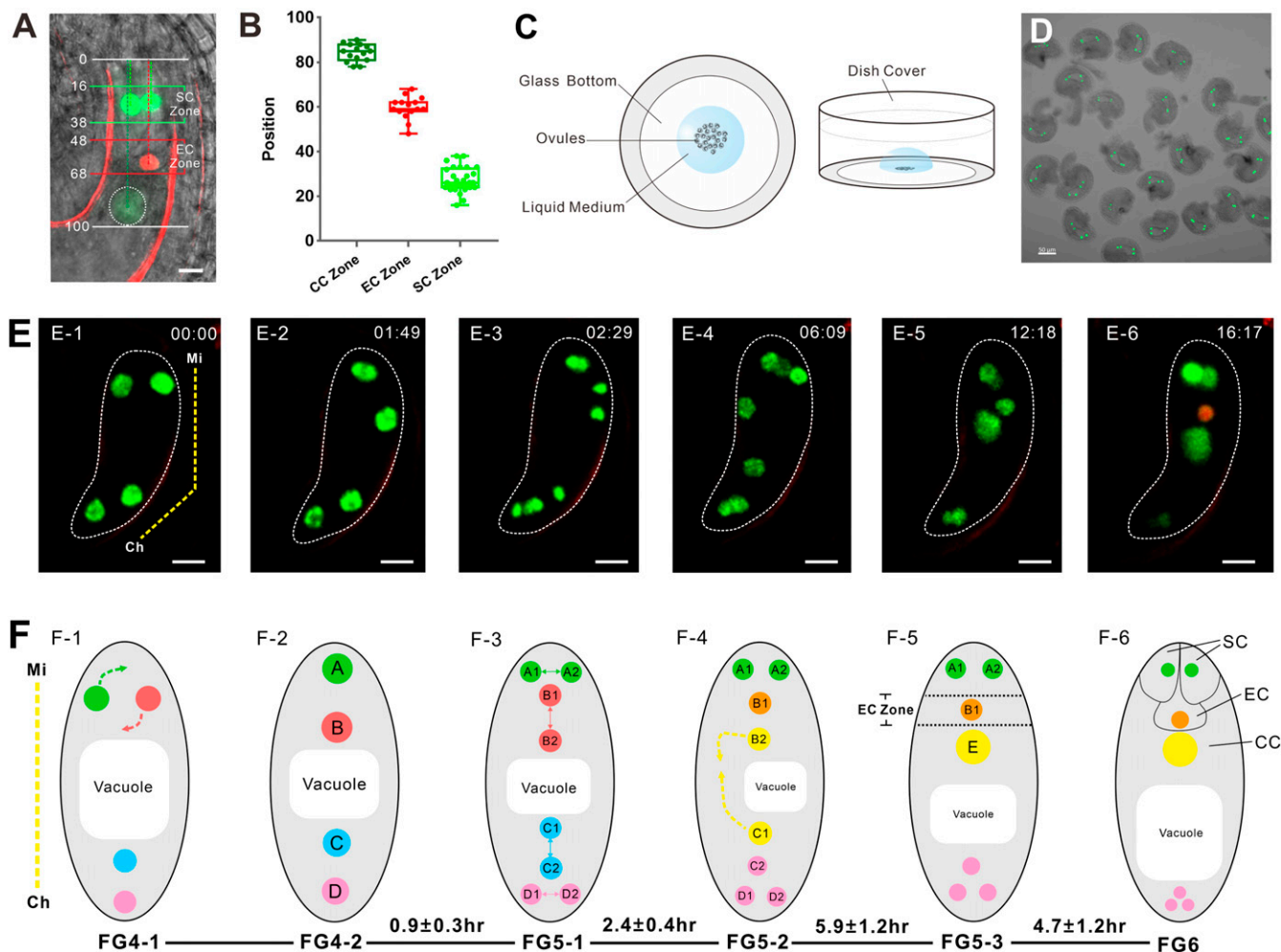


Fig. 1. The nucleus migrates to a specific position before cell specialization in the FG. (A) FGR7.0 is a triple marker line with RFP in the egg cell nucleus, bright GFP in synergid cell nuclei, and weak YFP in the central cell. In mature FGs, the nuclear positions of synergid cells are in the SC zone, the nuclear position of the egg cell is in the EC zone, and the nuclear position of the central cell is in the CC zone. The numbers are the relative positions of FGs. (Scale bar: 10 μm .) (B) Relative positions of the SC, EC, and CC zones. The data are calculated from ovules observed ($n = 15$). (C) Diagram of the in vitro ovule culture system. A Nitsch medium droplet containing ovules was added to the glass bottom of a cell culture dish. (Left) Top view. (Right) Front view. (D) A group of ovules at FG4 collected for culture. (Scale bar: 50 μm .) (E) Time lapse of NPCI FG development from FG4 to FG6. The yellow dotted line indicates the micropylar (Mi) end and the chalazal (Ch) end of the FG in E-1. The numbers in the right corner of each image are the culture times (h: min). In E-6, FG exhibits an egg cell. The whole process can be seen in *Movie S1*. (Scale bar: 10 μm .) (F) Diagram of FG development corresponding to E. The corresponding developmental stages and duration time (h) are indicated below the images. The duration time (mean \pm SD) was calculated from ovules observed ($n = 11$). The yellow dotted line indicates the Mi end and the Ch end of FG in F-1. The dotted arrows in F-1 show the direction of nuclear migration. In F-2, the four nuclei are arranged along the micropylar-chalazal axis and labeled as nuclei A, B, C, and D. In F-3, four nuclei divide to give rise to eight nuclei. Nuclei A1 and A2 are derived from nucleus A, nuclei B1 and B2 are derived from nucleus B, nuclei C1 and C2 are derived from nucleus C, and nuclei D1 and D2 are derived from nucleus D. In F-4, nuclei B2 and C1 move to each other. The dotted arrows show the direction of nuclear migration. In F-5, nuclei B2 and C1 fuse to form one large nucleus, E. Nucleus B1 is located in the EC zone. In F-6, the nucleus B1 shows an egg cell identity. Nuclei A1 and A2 located in the SC zone show synergid cell identity.

micropylar-chalaza axis (Fig. 1F-2). Approximately 40 min later, all four nuclei divided, giving rise to eight nuclei (stage FG5-1; Fig. 1E-3). Nuclei A1 and A2 were derived from nucleus A, located horizontally at the upper tier at the micropylar end. Nuclei B1 and B2 were derived from nucleus B located vertically at the lower tier at the micropylar end; nuclei C1 and C2 were derived from nucleus C, located horizontally in the upper tier at the chalazal end; and nuclei D1 and D2 were derived from nucleus D, located vertically in the lower tier at the chalazal end (Fig. 1F-3).

At ~6 h from stage FG4-1, two polar nuclei, B2 and C1, moved toward each other (stage FG5-2; Fig. 1E-4 and F-4). At ~12 h, these two polar nuclei merged together and fused into one large nucleus, E (stage FG5-3; Fig. 1E-5). At this time point, along the micropylar-chalazal axis, nuclei A1 and A2 were located horizontally in the SC zone, nucleus B1 was located in the EC zone, and the large nucleus E was located in the CC zone (Fig. 1F-5). The remaining three nuclei were located at the chalazal end. At ~16 h, the nucleus located in the EC zone displayed red fluorescence, indicating that the egg cell identity was established. The two nuclei located in the SC zone showed bright green fluorescence, indicating that the synergid cell fate was specified already (stage FG6; Fig. 1E-6 and F-6). This observation demonstrated that these cell identities were only established after the nuclei migrated to their specific position and did not occur immediately after nuclear formation in the FG.

Disruption of Nuclear Position Could Reset the Cell Identity of the Egg Apparatus. Since the nucleus positioning precedes cell specialization of the egg apparatus cells, we questioned whether the specific nuclear position is required for cell specialization. It is well known that nuclear movement is dependent on actin filaments in plants (24–27); thus, we used inhibitors of actin polymerization to alter the nuclear position in FGs. In the control (absence of inhibitor; $n = 79$), $77.4 \pm 7.9\%$ gametophytes progressed to stage FG6 (Fig. 2A). When the inhibitor of actin polymerization, latrunculin B (LATB), was used at a high concentration of 500 nM ($n = 75$), most of the gametophytes arrested at FG4 (Fig. 2C). When 250 nM LATB was used ($n = 106$), $12.5 \pm 2.6\%$ gametophytes progressed to stage FG6. Moreover, $3.1 \pm 2.7\%$ of the embryo sacs exhibited two nuclei in the EC zone with egg cell identity and only one in the SC zone with synergid cell identity. In the presence of 100 nM LATB ($n = 91$), $28.2 \pm 7.8\%$ of gametophytes progressed to stage FG6, and $5.9 \pm 2.7\%$ of the embryo sacs exhibited two nuclei in the EC zone with egg cell identity and only one nucleus in the SC zone with synergid cell identity (Fig. 2B). In the presence of 50 nM LATB ($n = 87$), no extra egg cells were detected. Treatment with an additional inhibitor of actin polymerization, cytochalasin B, also resulted in embryo sacs exhibiting two nuclei in the EC zone with egg cell identity and only one nucleus in the SC zone with synergid cell identity (SI Appendix, Fig. S2). These findings indicated that different positions were coupled with different cell identities.

We then investigated whether the nuclear position is also critical for cell identity in FG in vivo. A dominant negative mutant version of ACT8 (DN-ACT8) causes instability and fragmentation of actin filaments, leading to incomplete yet strong disruption of the actin cytoskeleton (25–29). We expressed DN-ACT8 under three FG-specific promoters—*ES1* (At5g40260), *ES2* (At1g26795), and *RH29* (At1g77030)—to disturb the actin filaments (24, 30). In all three types of transformed plants, there were FGs exhibiting two nuclei in the EC zone with egg cell identity and only one nucleus in the SC zone with synergid cell identity (Fig. 2F). In *proES2::DN-ACT8* ovules ($n = 389$), the ratio of FGs exhibiting two egg cells reached up to $10.1 \pm 2.4\%$ (Fig. 2E). In *proES1::DN-ACT8* ovules ($n = 366$) and *proRH29::DN-ACT8* ovules ($n = 412$), the ratio of ovules exhibiting two egg cells was $5.8 \pm 1.1\%$ and $6.1 \pm 1.2\%$, respectively (Fig. 2F).

To investigate whether the two cells exhibiting egg identity were indeed fully functional egg cells with an established female gamete cell fate, we pollinated the pistils of both the wild-type (WT) and *DN-ACT8* lines to observe fertilization and embryogenesis. In the WT ovule, a fertilized egg cell had divided and developed into an early globular embryo at 3 d after pollination (Fig. 2G), whereas at the same time in *DN-ACT8* line, both egg cells were fertilized and developed into two early globular embryos similar to their counterpart in the WT line (Fig. 2H). This result clearly demonstrates that the two egg cells with egg cell identity were fully functional female gametes.

To visualize the actin filaments in FG, we expressed the fluorescent reporter Lifeact-Tag-RFP (31, 32) under the control of the FG-specific *RH29* promoter (24). In WT, the actin cable could be clearly seen in FG (Fig. 2I–K). Consistent with the effect of DN-ACT8 reported previously, in the FG of *proES2::DN-ACT8* plants, the actin filaments became much shorter and generated aggregates (Fig. 2L–N). This modification of F-actin influenced nuclear migration and thus altered the final positions of the nuclei. The foregoing results indicate that the change in nuclear position on disruption of the actin cytoskeleton reset the cell identity of the egg apparatus.

Cell Fate Determination of the Egg Apparatus Depends on Its Final Position. To understand the origin of the additional egg cell, we monitored the whole development process of FGs from FG4 to FG6 in *proES2::DN-ACT8* plants using our live imaging system (SI Appendix, Fig. S3). Among the 91 monitored ovules, 38 (41.8%) FGs exhibited an abnormal mitosis pattern, in which the nuclear positions became abnormal from FG4 onward. The division plane of nucleus A was vertical in WT and oblique in transformed plants.

In 10 of the 91 monitored ovules (11.0%), FGs exhibited two egg cells, with the additional egg cell derived from either nucleus A2 or nucleus B2. In 6 cases (6.6%), nucleus B2 did not migrate to the CC zone but remained in the EC zone, while nucleus A2 migrated to the CC zone in FG5, resulting in nuclei B1 and B2 in the EC zone and only nucleus A1 in the SC zone at FG5-3. Approximately 6 h later, the two nuclei in the EC zone both showed egg cell identity, and nucleus A1 in the SC zone showed synergid identity (Fig. 3A and B). The whole process can be followed in Movie S2. The results indicate that nucleus B2, which was normally in the CC zone, stayed in the EC zone and thereafter had egg cell identity. In 4 other cases (4.4%), nucleus A2 migrated to the EC zone in FG5, resulting in both nucleus B1 and nucleus A2 in the EC zone, with only nucleus A1 in the SC zone at FG5-3. Approximately 8 h later, the two nuclei in the EC zone showed egg cell identity, and nucleus A1 in the SC zone displayed synergid identity. The whole process can be followed in Movie S3. The results indicate that nucleus A2, which should be in the SC zone, migrated to the EC zone and thereafter had egg cell identity (Fig. 3C and D).

In WT FGs and *proES2::DN-ACT8* FG with two egg cells, nucleus B1 consistently had an egg cell identity. It appeared that the egg cell fate was predetermined by the division of the precursor nucleus. However, unexpectedly, in 15 *proES2::DN-ACT8* FGs with one egg cell (16.5%), the nucleus B1 had synergid cell identity (Fig. 3E and F). In these cases, the two nuclei located horizontally at the micropylar end at FG4-1 did not turn to the vertical direction. The two nuclei divided, resulting in nuclei A1 and B1 located horizontally in the upper and nuclei A2 and B2 located horizontally in the lower tier (Fig. 3E-1 and E-2). Later, nuclei A1 and B1 were in the SC zone, while nucleus A2 was in the EC zone and nucleus B2 fused with nucleus C1 (Fig. 3E-3 and E-4). In mature FGs, nucleus A2 in the EC zone had egg cell identity, and nuclei B1 and A1 in the SC zone had synergid identity (Fig. 3E-5). The whole process can be followed in Movie S4. These results indicate that the determination of cell fate

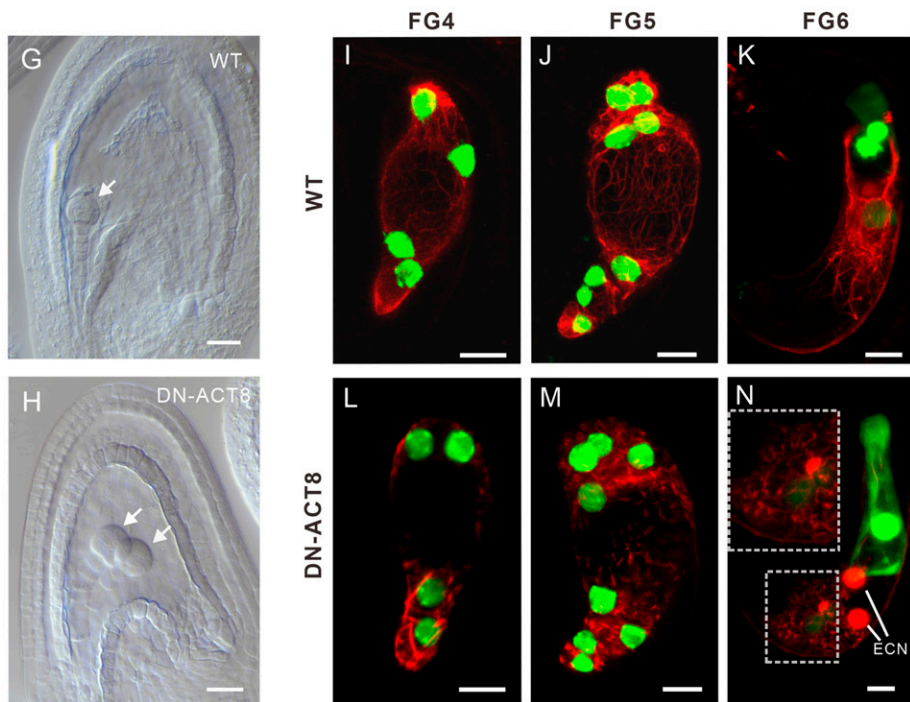
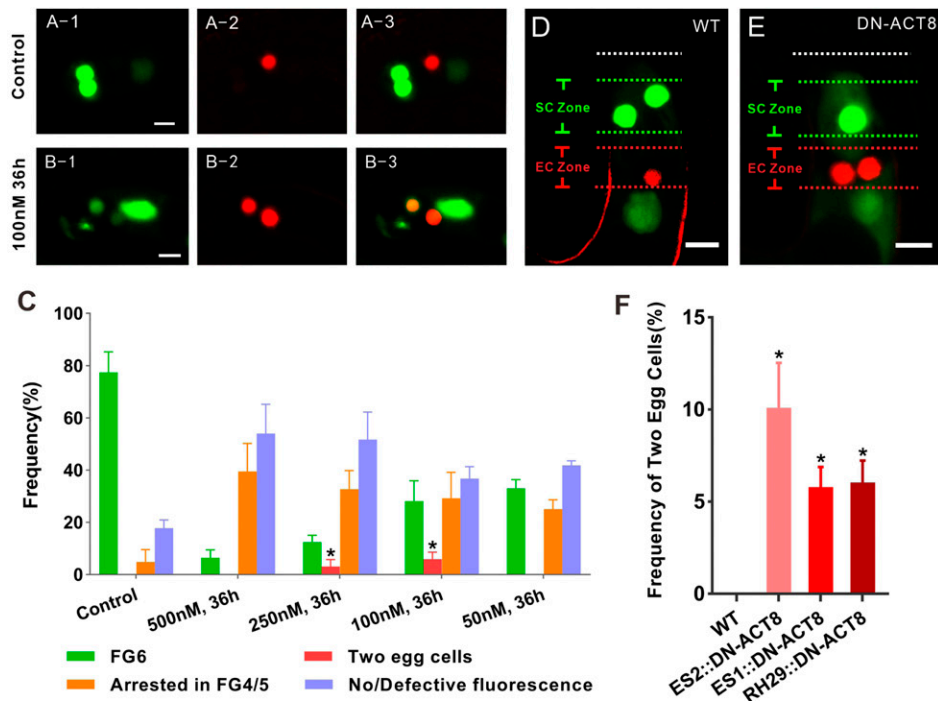


Fig. 2. Disruption of the nuclear position resets the cell identity of the egg apparatus. (A) In the control, there is only one egg cell. (B) Treatment with the inhibitor of actin polymerization LATB results in two egg cells. (C) LATB affects FG development and egg cell specialization. Ovules treated with a high concentration of LATB (500 nM) and FGs seldom develop to FG6, with most FGs arresting in FG4 or FG5 (FG4/5) or losing fluorescence. Treatment with 200 nM or 100 nM LATB, but not with 50 nM LATB, results in two egg cells. Most FGs develop to FG6 in the absence of LATB. At least three biological replicates were performed for each treatment, containing 15 to 26 ovules at FG4-1. The total number of ovules observed was 79, 75, 106, 91, and 87 for the control and 500 nM, 250 nM, 100 nM, and 50 nM LATB treatments, respectively. The data are mean \pm SD. Significant differences ($*P < 0.05$) were determined using the paired *t* test. (D) In WT, FGs contain two synergid cells and one egg cell at FG6 stage. (E) In transformed plants expressing DN-ACT8, FGs contain one synergid cell and two egg cells at FG6 stage. (F) Frequency of FGs exhibiting two egg cells in transformed plants expressing DN-ACT8. DN-ACT8 is expressed under the control of three FG-specific promoters—*ES1*, *ES2*, and *RH29*—to disturb actin filaments. The data (mean \pm SD) were counted from FG at FG6 stage of WT ($n = 245$), *ES1::DN-ACT8* ($n = 366$), *ES2::DN-ACT8* ($n = 389$), and *RH29::DN-ACT8* ($n = 412$). Significant differences ($*P < 0.05$) were determined using the paired *t* test. (G) In WT, there is a globular embryo at 3 d after fertilization. (Scale bar: 20 μ m.) (H) In the DN-ACT8 line, there are two globular embryos at 3 d after fertilization. (Scale bar: 20 μ m.) (I–K) In WT, the actin cable labeled by Lifeact-Tag-RFP can be clearly seen in FGs at FG4-FG6. (L–N) In *proES2::DN-ACT8* plants, the actin filaments became much shorter and generated aggregates in FG at FG4-FG6. In L, the FG at FG6 has two egg cells. The upper-left corner of the rectangle is an enlarged view of the lower-left of the rectangle, which shows that actin filaments are disrupted. (Scale bar: 10 μ m.)

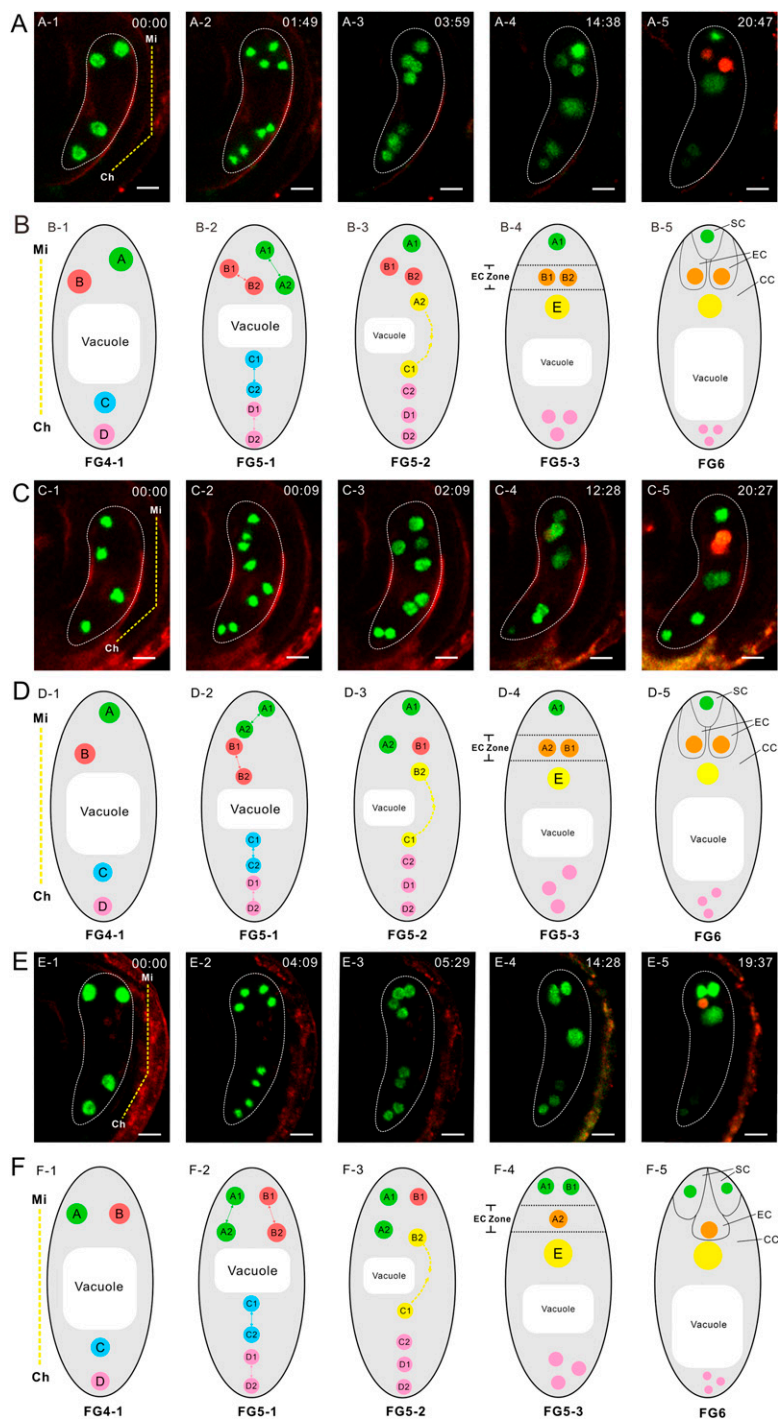


Fig. 3. Nuclear position determines the cell specialization of the egg apparatus. (A) Time lapse of FG development in *proES2::DN-ACT8* plants. The yellow dotted line in A-1 indicates the micropylar (Mi) end and chalazal (Ch) end of the FG. The numbers in each image are the culture times (h: min). In A-5, the FG has two egg cells. The whole process can be seen in [Movie S2](#). (B) Diagram of FG development corresponding to A. In B-1, the four nuclei arrange along the micropylar-chalazal axis and are labeled as nuclei A, B, C, and D. In B-2, four nuclei divide to give rise to eight nuclei. In B-3, nuclei A2 and C1 move to each other. The dotted arrows show the direction of nuclear migration. In B-4, nuclei A2 and C1 fuse to one large nucleus, E. Nuclei B1 and B2 are located in the EC zone. In B-5, nuclei B1 and B2 show red fluorescence. Nucleus A1 located in the SC zone shows bright green fluorescence. (C) Time lapse of FG development in *proES2::DN-ACT8* plants. The yellow dotted line in C-1 indicates the Mi end and the Ch end of FG. The numbers in each image are the culture times (h: min). In C-5, the FG has two egg cells. The whole process can be seen in [Movie S3](#). (D) Diagram of FG development corresponding to C. In D-1, the four nuclei arrange along the micropylar-chalazal axis and were labeled as nuclei A, B, C, and D. In D-2, four nuclei divide to give rise to eight nuclei. In D-3, nuclei B2 and C1 move to each other. In D-4, nuclei B2 and C1 fuse to one large nucleus, E. Nuclei B1 and A2 are located in the EC zone. In D-5, nuclei B1 and A2 show egg cell identity. The nucleus A1 located in the SC zone has synergid cell identity. (E) Time lapse of FG development in *proES2::DN-ACT8* plants. The yellow dotted line in E-1 indicates the Mi end and Ch end of the FG. The numbers in each image are the culture times (h: min). In E-5, FG has one egg cell. The whole process can be seen in [Movie S4](#). (F) Diagram of FG development corresponding to E. In F-1, the four nuclei were labeled as nuclei A, B, C, and D. In F-2, four nuclei divide to give rise to eight nuclei. In F-3, nuclei B2 and C1 move to each other. In F-4, nuclei B2 and C1 fuse to one big nucleus, E. Nuclei A1 and B1 are located in the SC zone. Nucleus A2 is located in the EC zone. In F-5, nucleus A2 shows egg cell identity. Nuclei A1 and B1 have synergid cell identity. (Scale bar: 10 μ m.)

depended on the final position in FGs at FG5 rather than on the specific nuclear lineage.

Auxin Plays a Role in Cell Type Specialization of the Egg Apparatus. A model has been proposed in which different levels of auxin within the embryo sac might determine cell fates (33). To investigate whether different distributions of auxin act as the positional cue to regulate egg apparatus specialization, we first detected the auxin level in the egg apparatus using the auxin sensor R2D2, a fluorescent reporter that allows the sensitive and semiquantitative readout of auxin responses at cellular resolution in *Arabidopsis*. This sensor comprises two components: an auxin-sensitive domain (DII:Venus) and a mutant version of DII (mDII:tdTomato) that serves as a control. A reduction in the DII:Venus signal indicates auxin accumulation (34). In WT, the DII:Venus signal was weaker in the egg cells than in the synergid cells (Fig. 4 A and B). Ratio analysis suggested higher auxin levels in egg cells compared with synergid cells (Fig. 4 C and D).

To investigate whether the higher auxin level in egg cells resulted from auxin transport, we treated ovules prior to FG6 with *N*-1-naphthylphthalamic acid (NPA), an auxin transport inhibitor. In control ovules without NPA treatment, the auxin level in the egg apparatus was consistent with that found in vivo (Fig. 4 E–H). Following NPA treatment, the auxin level was decreased in egg cells compared with synergid cells (Fig. 4 I–L).

To investigate the effect of auxin levels on cell specialization, we treated NPCI ovules from stage FG4 up to stage FG6 with NPA ($n = 109$). Interestingly, we found that in $9.0 \pm 3.9\%$ of NPA-treated ovules, the egg cell marker was no longer expressed (Fig. 4 N and O). Instead, three cells displayed synergid cell identity, with one cell occupying the position of the egg cell. This phenotype could not be detected in the control without NPA ($n = 86$). Our results suggest that auxin likely acted as a positional cue for egg apparatus specialization.

Discussion

It is well known that the nuclei of the cell in mature FGs have a specific position (Fig. 1 A and B), while how they migrate to their final position and the significance of this migration for cell differentiation remain unknown. The precise dynamics of FG development in *T. foeniculifer* were reported recently (22). In *T. foeniculifer*, the duration of final mitosis (FG4 to FG5) was 28 ± 6.5 min. In our live imaging system, the duration of final mitosis (FG4-2 to FG5-1) in *Arabidopsis* was 0.9 ± 0.3 h (Fig. 1F). In *T. foeniculifer*, the fusion of polar nuclei in the central cell occurred in ~ 13 h, and the onset of expression of LURE2, a pollen tube attractant, was visualized at ~ 11 h. In *Arabidopsis*, the fusion of polar nuclei in the central cell occurred at ~ 12 h, and the onset of FGR7.0 expression was visualized at ~ 16 h (Fig. 1E). The different dynamics of FG development may be related to different species or culture systems. Nevertheless, the live imaging system established by our group is a powerful tool for visualizing the live dynamics of nuclear position before cell specification in FGs. It revealed that in the WT, the four nuclei in FG4 have a stereotyped division pattern to produce eight nuclei (Fig. 1 E and F). Nuclei A1 and A2 migrate into the SC zone to specify their fates for a synergid cell, and nucleus B1 migrates into the EC zone to specify its fate for an egg cell later.

Whether the cell fates of the four types of the embryo sac component cells are determined in the three successive rounds of mitosis that occur in FGs and thus are determined by the cell lineage remains an unanswered question. According to our observations, nuclei of the same origin moved to different zones of the embryo sac and then showed different cell identities, whereas nuclei of different origins that moved to the same zone showed the same cell identity (Fig. 3). The nucleus that ends up within the egg cell zone at FG5 will transfer its cell fate to the egg cell,

suggesting a critical role of nuclear position rather than nuclear lineage in cell fate specification in FGs at FG5.

The hypothesis that nuclear position is important for cell fate specification in FGs was first suggested in *Zea mays*. In maize mutant *ig1* (INDETERMINATE GAMETOPHYTE 1), FGs undergo extra rounds of free nuclear divisions, resulting in supernumerary cells to produce extra synergid cells, egg cells, and central cells (35). Recently, the abnormal positioning of nuclei has been observed in some mutants with extra egg cells in *Arabidopsis* (15–20); however, how the extra egg cell forms is currently unknown. Researchers have suggested that the extra egg cell forms at the expense of the synergid cell. The live image system developed in the present study clearly showed that the extra egg cell either formed at the expense of the synergid cell or was a sister cell of the egg cell (Fig. 3 A–D and Movies S2 and S3). Moreover, whether nuclear position is the cause or the consequence of egg apparatus specification has remained unclear (21). Our results show that the change in nuclear position resulted in the change in egg apparatus specification (Fig. 3), indicating that nuclear position was the cause and the determining factor of egg apparatus specification.

The importance of specific positions of nuclei along the FG for cell fate determination might rely on the polar distribution of unknown determinants. One candidate determinant is CYTOKININ-INDEPENDENT 1 (CKI1). CKI1 can induce a typical cytokinin response and localize to the perinuclear endoplasmic reticulum of chalazal nuclei at the FG4 stage (36, 37). In *cki1*, central and antipodal cell fates are transformed into egg or synergid cell fate. Conversely, ectopic expression of CKI1 confers central cell identity to the cells in the position of synergid and egg cells (36). However, the synergid cells do not transform into egg cell fate in *cki1*, suggesting the presence of other determinants in FG or in the somatic tissue around FG.

Auxin is another candidate determinant. A model has been proposed in which different levels of auxin within the embryo sac might determine cell fate (33). Polarized DR5::GFP, an auxin-sensitive promoter that drives GFP as a marker for auxin concentration (38), was detected in the micropylar end of the embryo sac at FG5 in *Arabidopsis* (33). Overexpression of YUC1 to increase auxin synthesis expanded egg apparatus identity toward the chalazal pole (33), while extra egg cells at the micropylar pole of the FGs were observed in the *yuc1 yuc2* mutant line (33, 39), indicating the role of auxin in cell type differentiation in FGs. However, another group reported no detectable auxin gradient in the FGs of *Arabidopsis thaliana* and *Zea mays* (40). Therefore, it remains controversial whether there is sufficient bioactive auxin in FG for play a role in cell fate determination (33, 40). Of note, both groups used DR5 as a marker for the auxin concentration (33, 40). In our work, we used a new marker, R2D2, to monitor the auxin level, which is more sensitive than the classical DR5 marker (34). Our results showed that the auxin level was consistently higher in the egg cell than in synergid cells (Fig. 4 A–D), consistent with a previous report (41). Larsson et al. (41) detected the auxin level in *Arabidopsis* ovules using R2D2 and observed auxin accumulation and/or auxin-mediated activity in the unfertilized egg cells. We attempted to detect the auxin levels of FG at FG4 and FG5 with R2D2, but our attempts were fruitless due to problems imaging FG at the FG4/5 stage owing to interference of sporophytic signals in the R2D2 line. Although the time at which the egg cell has a higher auxin level than synergid cells is unclear, treatment with the auxin transport inhibitor NPA from FG4 could decrease the auxin level in egg cells (Fig. 4 I–L), indicating that auxin transport before FG6 is critical for auxin accumulation in egg cells. Furthermore, treatment with auxin transport inhibitor NPA could impair egg cell specialization (Fig. 4 M–O), indicating that a presence in the egg cell zone is not sufficient to cause egg cell fate when auxin transport is disrupted. Taken together, our results suggest that a

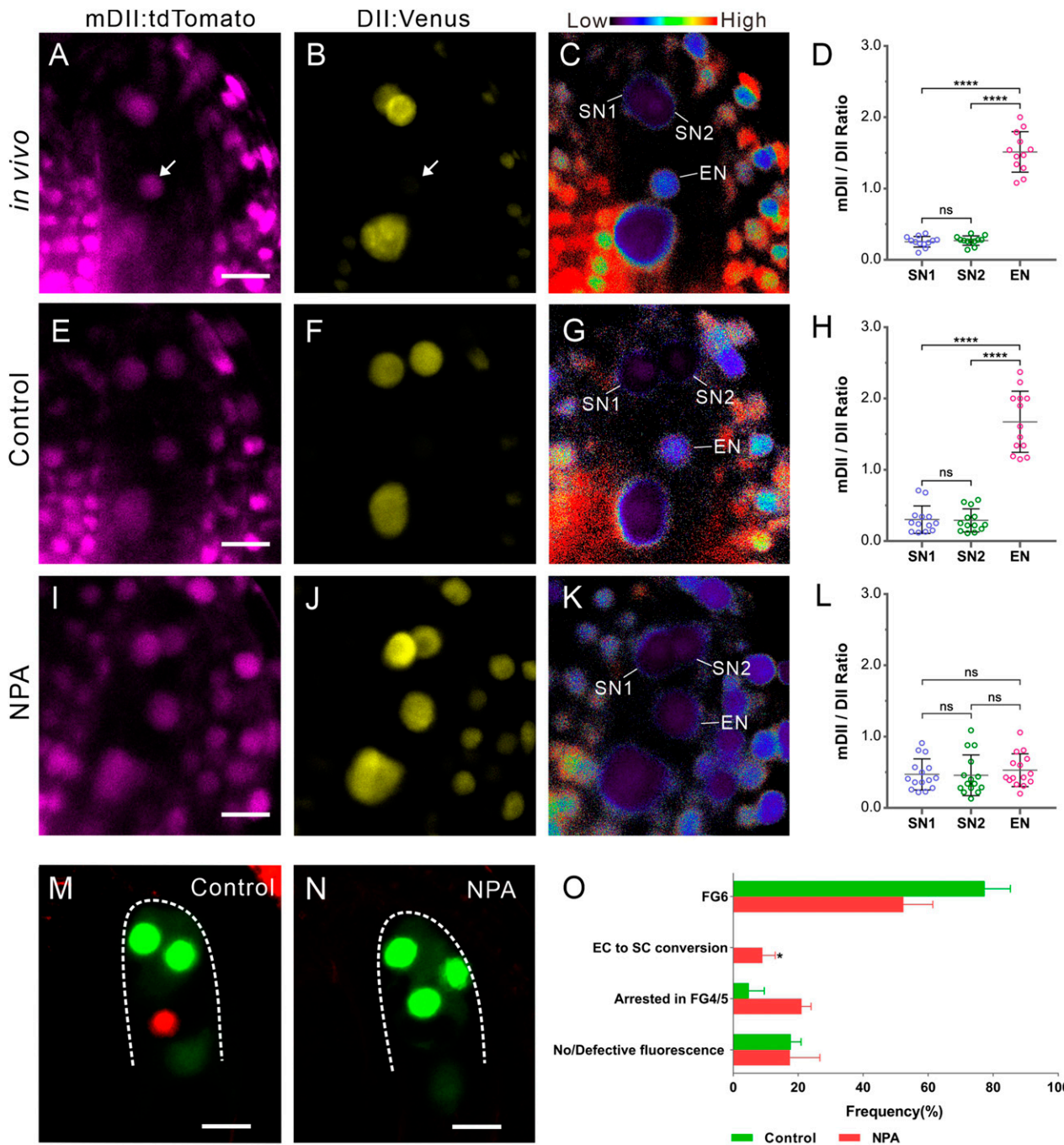


Fig. 4. Auxin affects cell specialization of the egg apparatus. (A and B) In vivo R2D2 signal at the micropylar end of FG at FG6 stage. R2D2 comprises two components: an auxin-sensitive domain (DII:Venus) and a mutant version of DII (mDII:tdTomato), which serves as a control. A reduction in the DII:Venus signal indicates auxin accumulation. (A) mDII:tdTomato signal. (B) A reduction in the DII:Venus signal at the egg cell nucleus indicates auxin accumulation. Arrows in A and B indicate the egg cell nucleus. (C) Ratio of mDII:tdTomato/DII:Venus signal in A and B. The ratio is displayed as false coloring according to the scale at the top, reflecting low to high auxin levels. The egg cell nucleus (EN) shows a higher auxin level than the two synergid cell nuclei (SN1 and SN2). (Scale bar: 10 μ m in A–C.) (D) R2D2 ratio statistics of the egg cell nucleus and synergid cell nucleus ($n = 12$ ovules). (E–H) In culture ovules without NPA treatment (controls), the R2D2 signal in the egg apparatus (E and F) is similar to that in vivo. The ratios of nuclei show a higher auxin level in EN than in SN1 and SN2 (G and H). (I–L) NPA treatment decreases the auxin level in the egg cell. Following NPA treatment, the mDII:tdTomato signal is similar to that in control (I), while no distinct reduction of the DII:Venus signal is detected in EN (J). The ratio of nuclei shows similar auxin levels among SN1, SN2, and EN (K and L). The R2D2 ratios were calculated from nuclei located in the egg apparatus, $n = 13$ and 15 ovules for the control and NPA treatment, respectively. The data in D, H, and L are mean \pm SD. Significant differences (**** $P < 0.0001$) and nonsignificant differences (ns, $P > 0.05$) were determined using the paired t test. (Scale bar: 10 μ m.) (M and N) The NPC1 marker shows cell specialization after treatment with the mock control and 200 μ M NPA. (M) In the mock control, there are two synergid cells with GFP fluorescence and one egg cell with RFP fluorescence. (N) After treatment with 200 μ M NPA, FGs cannot express the egg cell marker at stage FG6. Three cells express synergid GFP fluorescence. (Scale bar: 10 μ m.) (O) NPA treatment affects FG development and egg cell specialization. Ovules treated with 200 μ M NPA had enclosed FG at FG4-1. At least three biological replicates were performed for each treatment containing 16 to 23 ovules. The total number of ovules observed was 86 for control and 109 for NPA treatment. We found that 52.4 \pm 9.0% FGs could develop to FG6, 9.0 \pm 3.9% FGs contained three synergid cells but no egg cell (EC to SC conversion), and 38.6 \pm 7.9% FGs arrested in FG4 or FG5 (FG4/5) or lost fluorescence. The data are mean \pm SD. Significant differences (* $P < 0.05$) were determined using the paired t test.

directional and accurate auxin distribution likely acts as a positional cue for egg apparatus specialization.

Regardless of the positional cue, nuclear migration is a critical step in cell type differentiation. Migration of the nuclei is dependent on actin filaments, because a high concentration of LATB inhibits nuclear migration (Fig. 2C). Migration of the sperm nucleus to the egg cell nucleus or central cell nucleus in the embryo sac, as well as the nuclear movement in the zygote and its elongation, also depend on actin filaments (25–28), indicating that actin filaments play a major role in nuclear movement in reproductive cells. Therefore, the disruption of F-actin may provide a unique opportunity to monitor the positioning of nuclei and thus further investigate the effect of the positional cue on cell fate determination.

Materials and Methods

Plant Materials and Growth Conditions. The triple marker FGR7.0, a reporter that combines the marker genes for synergid cells, the egg cell, and the central cell on one plasmid (23), was kindly provided by Rita Groß-Hardt. The FG nucleus marker *proRH29::H2B-GFP* was described in our previous work (24). The auxin marker line R2D2 was kindly provided by Dolf Weijers (34). Seeds were surface-sterilized with 20% (vol/vol) bleach for 10 min and then washed three times with sterile distilled water. The seeds were stratified for 3 d at 4 °C and then sown on 1/2 Murashige and Skoog (MS) plates with 1.0% (wt/vol) sucrose. Agar plates were placed in a growth room with a 16-h light/8-h dark photoperiod. For selection, the medium was supplemented with 50 mg/L kanamycin (Sigma-Aldrich) or 50 mg/L hygromycin (Roche Diagnostics). Plants were grown in soil in a greenhouse under long-day conditions (16-h light/8-h dark) at 22 °C.

Plasmid Construction and Transgenic Plant Generation. All fragments were amplified by polymerase chain reaction (PCR) using the Phanta Kit (Vazyme Biotech). The primer sequences for PCR are listed in *SI Appendix, Table S1*, and all constructs were generated using restriction enzymes (New England Biolabs). The Lifeact-RFP and the dominant-negative form of ACTIN 8 (DN-ACT8) fragments were generated by overlap extension PCR (42). All constructs were transformed into *Agrobacterium tumefaciens* strain GV3101 and then into *Arabidopsis* plants by the floral dipping method (43).

In Vitro Ovule Culture System. To establish the culture system, we optimized the in vitro culture medium to improve the survival rate (44). The liquid medium contained Nitsch medium including vitamins (N0224.0050; Duchefa), 4% (wt/vol) trehalose dihydrate (563051; J&K Scientific), 1% (wt/vol) sucrose, and 0.3% (wt/vol) Pipes-KOH (pH 6.8). All the components were dissolved in double-distilled water for filtration sterilization. For the culture, the siliques were selected from flowers in development stage 12c and placed in the liquid medium droplets for dissection under a dissecting scope (1). The siliques were cut open along the replum with needles, and all the ovules at FG4 were carefully collected using a pipette and placed in a glass bottom cell culture dish (801001; Nest Biotechnology) containing a liquid medium droplet. All the ovules could gather in the center of a liquid medium droplet by slightly vibrating the dish to facilitate observation under the microscope.

Ovule Clearance. To observe the embryo phenotype, siliques at 3 d after pollination were dissected with needles and cleared in Herr's solution containing lactic acid:chloral hydrate:phenol:clove oil:xylene (2:2:2:1, wt/wt) as described previously (45). Images were acquired using a Nikon Ti2-A inverted microscope with differential interference contrast optics.

Microscopy. To image actin and embryo sacs within ovules, we used a laser-scanning confocal microscope (Leica SP8; 40×/1.3 NA objective lens) for

enhanced GFP (excitation, 488 nm; emission BP, 530 to 580 nm) and for RFP (excitation, 561 nm; emission BP, 600 to 650 nm). We used an inverted confocal microscope system (Zeiss LSM 880) for live imaging of FG development. The microscope was mounted on a Zeiss Axio Observer Z1 basic stand equipped with an incubator (XLMulti S1) to maintain the temperature at 22 °C. The Plan-Apochromat 20×/0.8 NA M27 objective (Zeiss) was used for imaging. Time-lapse images were acquired every 10 min using Z-stacks (9 to 12 steps, 1.8 to 2.2 μm each step) for 20 to 24 h. The laser excitation and filter were set for enhanced GFP and RFP using the settings detailed above. A Definite Focus unit was equipped to counteract drifting in the Z-direction. Image processing was performed with ZEN software (blue edition, Zeiss). For the R2D2 line, a 20×/0.75 NA objective (Leica SP8) was used for imaging. Venus was excited at 514 nm and detected at 524 to 540 nm; tdTomato was excited at 561 nm and detected at 571 to 630 nm. The mDII/DII ratio analysis was performed using Leica SP8 software as described previously (34).

Measurement of Cell Nucleus Position. To more clearly and accurately quantify the position of each nucleus in the embryo sac, we established a method to determine the position of the nucleus. First, the embryo sac close to the micropylar end was perpendicular to the horizontal line, and a horizontal line was made at the end of the micropylar end to set the position as 0. Subsequently, a horizontal line was made at the edge of the central cell nucleus to set it as 100. Next, the distance, D_{max} , between position 100 and position 0 and the distance, D_n , between the center of each nucleus and position 0 were measured using ImageJ, and the following formula was used to calculate position P_n of the nucleus in the embryo sac.

$$P_n = \frac{D_n}{D_{max}} \times 100.$$

Tracking Movement of the Cell Nucleus. To describe the movement of nuclei credibly and accurately, a set of time-lapse images for each FG was used to track the movement of nuclei frame by frame via a TrackMate tool in the ImageJ software. We developed the following rules to label the nuclei: 1) when the FG4 micropylar nuclei are not horizontally placed before the third mitosis, the nucleus located closer to the micropylar would be designated A (Figs. 1F and 3B and D); and 2) when the FG4 micropylar nuclei are placed horizontally before the third mitosis (Fig. 3E), the nucleus that produces the polar nucleus at micropylar region would be labeled B.

Inhibitor Treatment. To prepare the stock solution, LATB (ab144291; Abcam), cytochalasin B (S17006; Yuanye Bio-Technology), and NPA (33371; Sigma-Aldrich) were dissolved in DMSO to 1 mM, 20 mM, and 10 mM, respectively. For the inhibitor assay, the inhibitors were diluted in liquid medium to their working concentration before use. We used DMSO as a control for the medium containing inhibitors. Ovules were cultured at 22 °C in the dark for 24 to 36 h in an incubator. For inhibitor treatment in NPC1, ovules at FG4 stage could be collected according to the nuclear-located GFP signal. For NPA treatment in R2D2, there are limitations to collecting ovules at FG4 stage due to the interference of sporophytic signals in the R2D2 line. All cultured ovules were collected from siliques at flower development stage 12c, at which almost all the ovules were at FG4 or FG5 stage (1).

Data Availability. All study data are included in the main text and/or supporting information.

ACKNOWLEDGMENTS. We are grateful to Rita Groß-Hardt (University of Bremen) for providing the transgenic line FGR7.0 and Dolf Weijers (Wageningen University) for providing the transgenic line R2D2. This work was supported by the National Natural Science Foundation (31991201 and 31870302).

1. C. A. Christensen, E. J. King, J. R. Jordan, G. N. Drews, Megagametogenesis in *Arabidopsis* wild type and the Gf mutant. *Sex. Plant Reprod.* **10**, 49–64 (1997).
2. W. C. Yang, D. Q. Shi, Y. H. Chen, Female gametophyte development in flowering plants. *Annu. Rev. Plant Biol.* **61**, 89–108 (2010).
3. S. D. Russell, The egg cell: Development and role in fertilization and early embryogenesis. *Plant Cell* **5**, 1349–1359 (1993).
4. T. Higashiyama, The synergid cell: Attractor and acceptor of the pollen tube for double fertilization. *J. Plant Res.* **115**, 149–160 (2002).
5. J. Ning *et al.*, Differential gene expression in egg cells and zygotes suggests that the transcriptome is restructured before the first zygotic division in tobacco. *FEBS Lett.* **580**, 1747–1752 (2006).
6. S. Okuda *et al.*, Defensin-like polypeptide LUREs are pollen tube attractants secreted from synergid cells. *Nature* **458**, 357–361 (2009).

7. S. Sprunck, U. Baumann, K. Edwards, P. Langridge, T. Dresselhaus, The transcript composition of egg cells changes significantly following fertilization in wheat (*Triticum aestivum* L.). *Plant J.* **41**, 660–672 (2005).
8. T. Ohnishi *et al.*, Distinct gene expression profiles in egg and synergid cells of rice as revealed by cell type-specific microarrays. *Plant Physiol.* **155**, 881–891 (2011).
9. S. Okuda, T. Higashiyama, Pollen tube guidance by attractant molecules: LUREs. *Cell Struct. Funct.* **35**, 45–52 (2010).
10. R. D. Kasahara, M. F. Portereiko, L. Sandaklie-Nikolova, D. S. Rabiger, G. N. Drews, MYB98 is required for pollen tube guidance and synergid cell differentiation in *Arabidopsis*. *Plant Cell* **17**, 2981–2992 (2005).
11. A. Capron *et al.*, Maternal control of male-gamete delivery in *Arabidopsis* involves a putative GPI-anchored protein encoded by the LORELEI gene. *Plant Cell* **20**, 3038–3049 (2008).

12. J. M. Escobar-Restrepo *et al.*, The FERONIA receptor-like kinase mediates male-female interactions during pollen tube reception. *Science* **317**, 656–660 (2007).
13. C. Li *et al.*, Glycosylphosphatidylinositol-anchored proteins as chaperones and co-receptors for FERONIA receptor kinase signaling in Arabidopsis. *eLife* **4**, e06587 (2015).
14. S. Sprunck *et al.*, Egg cell-secreted EC1 triggers sperm cell activation during double fertilization. *Science* **338**, 1093–1097 (2012).
15. R. Gross-Hardt *et al.*, LACHESIS restricts gametic cell fate in the female gametophyte of Arabidopsis. *PLoS Biol.* **5**, e47 (2007).
16. O. Kirioukhova *et al.*, Female gametophytic cell specification and seed development require the function of the putative Arabidopsis INCENP ortholog WYRD. *Development* **138**, 3409–3420 (2011).
17. J. Kong, S. Lau, G. Jürgens, Twin plants from supernumerary egg cells in Arabidopsis. *Curr. Biol.* **25**, 225–230 (2015).
18. C. Moll *et al.*, CLO/GFA1 and ATO are novel regulators of gametic cell fate in plants. *Plant J.* **56**, 913–921 (2008).
19. G. C. Pagnussat, H. J. Yu, V. Sundaresan, Cell-fate switch of synergid to egg cell in Arabidopsis eostre mutant embryo sacs arises from misexpression of the BEL1-like homeodomain gene BLH1. *Plant Cell* **19**, 3578–3592 (2007).
20. R. Völz *et al.*, LACHESIS-dependent egg-cell signaling regulates the development of female gametophytic cells. *Development* **139**, 498–502 (2012).
21. I. Erbasol Serbes, J. Palovaara, R. Groß-Hardt, Development and function of the flowering plant female gametophyte. *Curr. Top. Dev. Biol.* **131**, 401–434 (2019).
22. D. Susaki, H. Takeuchi, H. Tsutsui, D. Kurihara, T. Higashiyama, Live imaging and laser disruption reveal the dynamics and cell-cell communication during *Torenia fournieri* female gametophyte development. *Plant Cell Physiol.* **56**, 1031–1041 (2015).
23. R. Völz, J. Heydlauff, D. Ripper, L. von Lyncker, R. Groß-Hardt, Ethylene signaling is required for synergid degeneration and the establishment of a pollen tube block. *Dev. Cell* **25**, 310–316 (2013).
24. D. Chen *et al.*, Gametophyte-specific DEAD-box RNA helicase 29 is required for functional maturation of male and female gametophytes in Arabidopsis. *J. Exp. Bot.* **71**, 4083–4092 (2020).
25. T. Kawashima *et al.*, Dynamic F-actin movement is essential for fertilization in Arabidopsis thaliana. *eLife* **3**, e04501 (2014).
26. Y. Ohnishi, T. Okamoto, Karyogamy in rice zygotes: Actin filament-dependent migration of sperm nucleus, chromatin dynamics, and de novo gene expression. *Plant Signal. Behav.* **10**, e989021 (2015).
27. Y. Ohnishi, T. Okamoto, Nuclear migration during karyogamy in rice zygotes is mediated by continuous convergence of actin meshwork toward the egg nucleus. *J. Plant Res.* **130**, 339–348 (2017).
28. X. Peng, T. Yan, M. Sun, The WASP-Arp2/3 complex signal cascade is involved in actin-dependent sperm nuclei migration during double fertilization in tobacco and maize. *Sci. Rep.* **7**, 43161 (2017).
29. T. Kato, M. T. Morita, M. Tasaka, Defects in dynamics and functions of actin filament in Arabidopsis caused by the dominant-negative actin fiz1-induced fragmentation of actin filament. *Plant Cell Physiol.* **51**, 333–338 (2010).
30. H. J. Yu, P. Hogan, V. Sundaresan, Analysis of the female gametophyte transcriptome of Arabidopsis by comparative expression profiling. *Plant Physiol.* **139**, 1853–1869 (2005).
31. J. Riedl *et al.*, Lifeact: A versatile marker to visualize F-actin. *Nat. Methods* **5**, 605–607 (2008).
32. A. Era *et al.*, Application of Lifeact reveals F-actin dynamics in Arabidopsis thaliana and the liverwort, *Marchantia polymorpha*. *Plant Cell Physiol.* **50**, 1041–1048 (2009).
33. G. C. Pagnussat, M. Alandete-Saez, J. L. Bowman, V. Sundaresan, Auxin-dependent patterning and gamete specification in the Arabidopsis female gametophyte. *Science* **324**, 1684–1689 (2009).
34. C. Y. Liao *et al.*, Reporters for sensitive and quantitative measurement of auxin response. *Nat. Methods* **12**, 207–210 (2015).
35. F. Guo, B. Q. Huang, Y. Han, S. Y. Zee, Fertilization in maize indeterminate gametophyte1 mutant. *Protoplasma* **223**, 111–120 (2004).
36. L. Yuan *et al.*, The CK1I histidine kinase specifies the female gametic precursor of the endosperm. *Dev. Cell* **37**, 34–46 (2016).
37. T. Kakimoto, CK1I, a histidine kinase homolog implicated in cytokinin signal transduction. *Science* **274**, 982–985 (1996).
38. T. Ulmasov, J. Murfett, G. Hagen, T. J. Guilfoyle, Aux/IAA proteins repress expression of reporter genes containing natural and highly active synthetic auxin response elements. *Plant Cell* **9**, 1963–1971 (1997).
39. A. Panoli *et al.*, Auxin import and local auxin biosynthesis are required for mitotic divisions, cell expansion and cell specification during female gametophyte development in Arabidopsis thaliana. *PLoS One* **10**, e0126164 (2015).
40. D. S. Lituiev *et al.*, Theoretical and experimental evidence indicates that there is no detectable auxin gradient in the angiosperm female gametophyte. *Development* **140**, 4544–4553 (2013).
41. E. Larsson, A. Vivian-Smith, R. Offringa, E. Sundberg, Auxin homeostasis in Arabidopsis ovules is anther-dependent at maturation and changes dynamically upon fertilization. *Front. Plant Sci.* **8**, 1735 (2017).
42. R. M. Horton, In vitro recombination and mutagenesis of DNA: SOEing together tailor-made genes. *Methods Mol. Biol.* **15**, 251–261 (1993).
43. S. J. Clough, A. F. Bent, Floral dip: A simplified method for agrobacterium-mediated transformation of Arabidopsis thaliana. *Plant J.* **16**, 735–743 (1998).
44. K. Gooh *et al.*, Live-cell imaging and optical manipulation of Arabidopsis early embryogenesis. *Dev. Cell* **34**, 242–251 (2015).
45. Y. H. Ding, N. Y. Liu, Z. S. Tang, J. Liu, W. C. Yang, Arabidopsis GLUTAMINE-RICH PROTEIN23 is essential for early embryogenesis and encodes a novel nuclear PPR motif protein that interacts with RNA polymerase II subunit III. *Plant Cell* **18**, 815–830 (2006).